The Oldest Stars of the Extremely Metal-Poor Local Group Dwarf Irregular Galaxy Leo A[1]

Regina E. Schulte-Ladbeck

University of Pittsburgh, Pittsburgh, PA 15260, USA

rsl@phyast.pitt.edu

Ulrich Hopp

Universitätssternwarte München, München, FRG

hopp@usm.uni-muenchen.de

Igor O. Drozdovsky

University of Pittsburgh, Pittsburgh, PA 15260, USA, and University of St. Petersburg, St. Petersburg, Russia

dio@phyast.pitt.edu

Laura Greggio

Osservatorio Astronomico di Bologna, Bologna, Italy, and Universitätssternwarte München, München, FRG

greggio@usm.uni-muenchen.de

Mary M. Crone

Skidmore College, Saratoga Springs, NY 12866, USA

[1]Based on observations made with the NASA/ESA Hubble Space Telescope obtained from the Space Telescope Science Institute, which is operated by the Association of Universities for Research in Astronomy, Inc., under NASA contract NAS 5-26555.

mcrone@skidmore.edu

Received _____; accepted _____

ABSTRACT

We present deep Hubble Space Telescope single-star photometry of Leo A in B, V, and I. Our new field of view is offset from the centrally located field observed by Tolstoy et al. (1998) in order to expose the halo population of this galaxy. We report the detection of metal-poor red horizontal branch stars, which demonstrate that Leo A is not a young galaxy. In fact, Leo A is as least as old as metal-poor Galactic Globular Clusters which exhibit red horizontal branches, and are considered to have a minimum age of about 9 Gyr. We discuss the distance to Leo A, and perform an extensive comparison of the data with stellar isochrones. For a distance modulus of 24.5, the data are better than 50% complete down to absolute magnitudes of 2 or more. We can easily identify stars with metallicities between 0.0001 and 0.0004, and ages between about 5 and 10 Gyr, in their post-main-sequence phases, but lack the detection of main-sequence turnoffs which would provide unambiguous proof of ancient (>10 Gyr) stellar generations. Blue horizontal branch stars are above the detection limits, but difficult to distinguish from young stars with similar colors and magnitudes. Synthetic color-magnitude diagrams show it is possible to populate the blue horizontal branch in the halo of Leo A. The models also suggest ≈50% of the total astrated mass in our pointing to be attributed to an ancient (>10 Gyr) stellar population. We conclude that Leo A started to form stars at least about 9 Gyr ago. Leo A exhibits an extremely low oxygen abundance, of only 3% of Solar, in its ionized interstellar medium. The existence of old stars in this very oxygen-deficient galaxy illustrates that a low oxygen abundance does not preclude a history of early star formation.

Subject headings: Galaxies: irregular — galaxies: dwarf — galaxies: individual (Leo A = UGC 5364 = DDO 69) — galaxies: stellar content

1. Introduction

The ages of dwarf galaxies provide an important test of galaxy formation models. Galaxy formation through bottom-up gravitational collapse implies that small halos tend to form earliest. While many merge to form more massive halos, small halos which have escaped merging may still be found today, and in large numbers (e.g. Klypin et al. 1999, White & Springel 2000, Marzke & Da Costa 1997, Ellis 1997). As the surviving building blocks of the large galaxies, today's dwarf galaxies may have been hosts of the earliest star formation in the Universe.

But there are also reasons one might expect to see nearby dwarf galaxies with no old stars. First, low-mass halos in the early Universe were not necessarily effective at collecting gas, or at allowing gas to cool and experience star formation. For instance, star formation in low-mass halos may be effectively quenched by supernovae from the first burst, or delayed by the high UV background at re-ionization (e.g. Dekel & Silk 1986, Babul & Ferguson 1996, Ferrara & Tolstoy 2000, Barkana & Loeb 2001). Second, some small-scale density perturbations may have become non-linear only recently, furnishing additional young, late-formed halos in the present epoch (e.g. Roukema et al. 1997). Theory thus predicts a wide range of formation ages for the first stars in dwarf galaxies.

There is yet another possible formation history for dwarf galaxies. The more metal-rich, tidal dwarfs appear to result from galaxy mergers (e.g. Duc & Mirabel 1998), and can therefore form over an extended time period.

On the observational side, it is already clear that the dwarf galaxies of the Local Group have experienced diverse star-formation histories (SFH) (e.g. Mateo 1998, 2000). All well-studied dwarf Spheroidal (dSph) galaxies of the Local Group contain stars at least 10 Gyr old, as evidenced by main-sequence turn-off (MSTO) stars with luminosities similar to those in old Galactic globular clusters (GC), the presence of RR Lyrae variables, and the

presence of extended horizontal branches (HB) (e.g. Mateo 2000). DSphs with extended HBs often exhibit a population gradient: the higher-mass, red HB (RHB) stars are more concentrated toward the center while the lower-mass, blue HB (BHB) stars dominate at large distances (Harbeck et al. 2001). However, whether or not ancient stellar populations are also ubiquitous in actively star-forming dwarfs, such as dwarf Irregular (dIrr) or Blue Compact Dwarf (BCD) galaxies (of which there are no examples within the Local Group), is not yet clear. Population gradients in the young stellar component are clearly seen in dIrrs (e.g. Minniti & Zijlstra 1996, Grebel 1999) and BCDs (e.g. Schulte-Ladbeck et al. 1999, Tosi et al. 2001), but only for the most nearby dIrrs does current instrumentation permit the direct observation of old stars.

Evidence for ancient stars in dIrrs, while as yet scarce, does exist. RR Lyrae stars have been detected in IC 1613 (Saha et al. 1992). WLM contains a globular cluster whose color-magnitude diagram (CMD) is similar to those of old, Galactic GCs (Hodge et al. 1999). The field populations of IC 1613 and of WLM exhibit a BHB (Cole et al. 1999, Rejkuba et al. 2000), and are considered to be an ancient stellar substratum.

In contrast, Leo A (= UGC 5364 = DDO 69) might represent a delayed-formation dwarf galaxy. Tolstoy et al. (1998) obtained a CMD of Leo A with HST/WFPC2, and found that the dominant stellar population in their centrally located field of view is less than about 2 Gyr old. They cautiously termed Leo A a "predominantly young galaxy" in the Local Group. Confirming the existence of a truly young galaxy in the present epoch would have a great impact on our understanding of galaxy formation, and motivates the research presented in this paper.

Interestingly, Leo A is also the most metal-poor (i.e. oxygen-poor) galaxy of the Local Group. After the BCDs I Zw 18 and SBS 0335-032, it is the third most oxygen-poor star-forming galaxy known today (a place it shares with UGCA 292). Its interstellar

medium (ISM) has an O abundance of only 3% of Solar (12+log(O/H) = 7.30, Skillman, Kennicutt & Hodge 1989, van Zee, Skillman & Haynes 1999), almost as low as the famous I Zw 18, which is at 2% of Solar. At the same time, Leo A is about a factor of 15—30 closer, allowing its stellar content to be resolved to deeper limits.

Tolstoy et al. (1998) presented HST/WFPC2 observations down to about 25.5 to 26 in B, V & I. They found that the CMDs of Leo A are consistent with a formation time less than 2 Gyr ago. Specifically, their arguments are:

1. A horizontal branch, the signpost of an old stellar population in GCs and dSphs, is not observed.

2. The narrow red-giant branch (RGB) is consistent with a young (1—2 Gyr) age and little prior enrichment (if there were any older stars that enriched the gas), and so is the ratio of red clump (RC) to RGB stars.

3. The red giants do not extend spatially beyond the main-sequence (MS) stars, so there is no "Baade's red sheet", the classical morphological indicator of a Pop II.

Since a small (10%), underlying old ($\geq$ 10 Gyr) population could not be ruled out, the authors cautiously call Leo A a "predominantly young galaxy" in the Local Group.

The unique nature of Leo A justified additional, and much deeper, HST observations. We requested to obtain single-star photometry down to V$\approx$28 in the *halo* of Leo A, for the following reasons. First, Tolstoy et al. observed on the main body of Leo A. Their Figs. 5 & 6 show the CMDs of the main body, using broad B, V & I bands. The B,V data are near the photometric limits where one would expect to see the RHB. Their B,V and V,I CMDs show that any BHB is completely confused by the young stellar population. A detection of the HB stars may however be possible with deeper imaging and at large

galactocentric distance. At larger distances from the center, there might be less of a young stellar population, resulting also in less crowding and blending of stellar images. Second, Tolstoy et al. argued that there is no spatial segregation between the MS and the RGB stars, based on the fact that MS stars are also seen in the outer regions of their data. On its digitized sky survey (DSS) image, the outer isophotes of Leo A extend well beyond the area covered by the Tolstoy et al. observations. In fact, Demers et al. (1984) find that the Holmberg diameter of Leo A is 7'. A pointing at large distance might reveal "Baade's red sheet", a population of old red giants, in addition to the old HB stars[2]. Therefore, in order to clarify unambiguously whether or not Leo A is a young galaxy, we obtained new HST/WFPC2 data in a field further removed from the young populations. Based on the new data, we make the case that stars with ages of at leat 9 Gyr, and possibly greater, are present in Leo A. Therefore, its age of formation is similar to other galaxies in the Local Group for which deep single-star photometry is available.

2. Observations

Figure 1 shows the locations of the Tolstoy et al. pointing and our pointing. The position of Leo A in RA, Dec (2000) is $09^h59^m26^s$, $+30^o44'47"$ (Cotton, Condon & Arbizzani 1999). The center of the Tolstoy et al. pointing was at $09^h59^m27^s$, $+30^o44'22"$, whereas our pointing was centered at $09^h59^m33^s$, $+30^o43'40"$, and had a roll angle which positioned much of the WF chips into the outskirts of Leo A.

[2]Dolphin et al. (2002) recently showed stellar density maps based on gound-based photometry which indicate the red-giant-star distribution is larger than that of bright blue plume stars.

2.1. The Data

Our observations were gathered as part of GO program 8575. We obtained dithered exposures in three filters, with total exposure times of 22,200s in F439W, and 8,300s each in F555W and F814W.

The data reduction included the usual post-pipeline reductions and used the zero points from the May 1997 SYNPHOT tables. We performed single-star photometry with DAOPHOT II (Stetson 1994) to obtain photometry in instrumental magnitudes (in the HST Vegamag system). We also transformed them to ground-based Johnson-Cousins B, V, I magnitudes with the help of Holtzman et al. (1995). The chips which we are most interested in are the ones farthest away from the center of Leo A; we performed ADDSTAR tests on chips WF3 and WF4, and found that completeness is high well down to the RC. Very few Galactic foreground stars are expected due to the high latitude of Leo A and the small field of view of the WFPC2 (see Tolstoy et al.). No internal extinction is apparent in color-color diagrams of our data. We adopt the foreground extinction of Schlegel, Finkbeiner & Davis (1998, and see NED), namely A_B=0.089, A_V=0.068, and A_I=0.040 (slightly different from that used by Tolstoy et al.). In Fig. 2, we show CMDs in [(F439W-F555W)$_0$, F555W$_0$], [(F555W-F814W)$_0$, F814W$_0$], and [(F439W-F814W)$_0$, F814W$_0$] for each individual WFPC2 chip.

Most of the CMDs we discuss below use photometry transformed into B, V, and I. Therefore, we give in Figs. 3 & 4 DAOPHOT photometric errors and completeness fractions in B, V & I, for both the WF3 and WF4 chips.

The Tolstoy et al. HST photometry reached estimated errors of 0.2 mag for B≈25.5, V≈26.5, and I≈25.5. Our data go about 2 mag. fainter for similar errors.

2.2. CMD Characteristics

We detect a total of 4747 stars in B and V; 4136 in V and I; and 3704 in B, V, and I. For comparison, in the Tolstoy et al. data set there are 2636 stars in B and V, and 7295 stars in V and I. Although our data go to deeper limiting magnitudes than the Tolstoy et al. data, our [V-I, I] set nevertheless contains a much smaller number of point sources. This can be understood in terms of a lower stellar density toward larger galactocentric radii, also seen in Fig. 1.

Figure 2 presents the CMDs for each chip in three different filter combinations. The CMDs of all four chips exhibit blue and red plumes. The blue plume consists of MS stars of a wide mass range, blue supergiant (BSG), and blue-loop (BL) stars. The BL stars are core-He burning descendants of massive and intermediate-mass stars, and are also evident as bright stars between the two plumes. Subgiant branch (SGB) stars of lower-mass contribute to widen the bottom of the blue plume. The red plume contains very few luminous red supergiant (RSG) and bright or thermally-pulsing asymptotic giant branch (AGB) stars, but a well-developed RGB/AGB branch. Note the well-populated RC in all four chips and in all CMDs. The RC area of the CMDs contains a mix of core-He burners with intermediate and low masses. At its bright and blue edge, there is a contribution from intermediate-mass BL stars, whereas at the faint and blue edge, there is a spur of low-mass RHB stars. The RC area is in part superimposed on the RGB and AGB. These two branches consist of intermediate- and low-mass H-shell burning stars which evolve up the RGB, as well as double-shell burning intermediate- and low-mass stars which ascend for a second time after core-He exhaustion.

The two plumes merge toward faint magnitudes. This is attributed to the detection of subgiant branches of intermediate-mass stars after core-H exhaustion plus scatter due to increasing photometric errors and blending for fainter sources.

2.3. Population Changes with Radius

Figure 2 illustrates that the stellar content of Leo A varies with position (compare Fig. 1 for the locations of the chips relative to the body of Leo A). We concentrate on comparing starcounts on the WF chips; starcounts on the PC chip, with its different area and sensitivity, are not directly comparable to those on the WF chips.

Fig. 2a best shows the variation in the MS component as a function of galactocentric distance. The blue plume on WF2 is seen to be very well populated at bright magnitudes. MS stars are much less abundant, and the brightness of the bulk of MS stars becomes fainter, on WF3 and 4. Fig. 2c illustrates that another relatively young stellar component, the BL stars, are quite prominent on WF2, and readily apparent on WF4, but rare on WF3. The morphology of the RC also changes. This is best seen in Fig. 2c. On WF2 and 4, the RC has a contribution of stars brighter than 24^{th} magnitude, which make it appear round. On WF3, these bright stars are missing, and the RC morphology is that of a narrow triangle with the long side defined by stars with colors of (F439W-F814W)$_0 \approx 1$. This blue part of the RC is clearly made up of HB stars, the lowest-mass and hence oldest stars which can be distinguished on our CMDs.

The stellar population changes with radius can also be illustrated with the help of chip-by-chip luminosity functions (LF). The changes in the young stellar content with radius are best seen in the V-band LF. In Fig. 5a, we show the F555W$_0$ LF for all stars with (F439W-F555W)$_0 \leq 0$. The top of the MS, defined as the magnitude at which the F555W$_0$ LF first systematically rises above zero, occurs at 23.0±0.1 on WF2, 25.3±0.2 on WF4, and 25.5±0.1 on WF3. The increase in stellar density just below magnitude 25 on WF3 & WF4 could also be due to a large relative contribution by BHB stars.

Starcounts on the [(F439W-F555W)$_0$, F555W$_0$] CMDs along the top of the blue plume with limits $20 <$ F555W$_0 < 25$ (where the faint limit is set by the onset of a potential BHB

contribution) and (F439W-F555W)$_0 \leq 0$, yield 194±14 bright blue stars on WF2, 24±5 on WF4, and 18±4 on WF3 (the "errors" are $\sqrt{N}$). This corresponds to relative numbers of bright, blue-plume stars on the WF chips in proportions 1 : 0.12 : 0.09. From Fig. 2b, we see that BL stars occupy the region $20 <$ F814W$_0 < 24$ and $0 <$ (F555W-F814W)$_0 < 0.6$. We find 48±7 stars on WF2, 18±4 on WF4, and 7±3 on WF3, or BL stars in ratios of 1 : 0.38 : 0.15. The LFs and the CMDs thus indicate a strong gradient in the number density of young stars with distance from the center of Leo A.

The changes in the intermediate-age/old stellar content with radius are best seen in the I-band LF. Fig. 5b shows chip-by-chip LFs for the red plume. They were constructed from the [(F555W-F814W)$_0$, F814W$_0$] CMDs with color selection criterion $0.65 <$ (F555W-F814W)$_0 < 1$. A small, gradual decrease in stellar numbers from WF2, to WF4, to WF3, is apparent. This indicates changes in the numbers of RC and RGB/AGB stars, but at a much smaller rate than the change seen in the young, MS component. Counting stars in the top mangitudes of the RGB/AGB on the [(F555W-F814W)$_0$, F814W$_0$] CMDs with $19.5 <$ F814W$_0 < 23$ and $0.8 <$ (F555W-F814W)$_0 < 2$, we find 54±7 on WF2, 53±7 on WF4, and 27±5 on WF3, or relative numbers of 1 : 0.98 : 0.5. When we define the area of the RC to encompass stars with $23 <$ F814W$_0 < 24.5$ and $0.6 <$ (F555W-F814W)$_0 <$ 1.2, we count 287±17 stars on WF2, 236±15 on WF4, and 185±14 WF3, or ratios of 1 : 0.82 : 0.64. This supports the visual impression of a less rapid change with distance in the intermediate-age/old as compared to the young stellar component.

The RC also changes in morphology. This can best be seen in Figs. 2c. At the same time (as seen e.g. on Fig. 5b), the RC LF appears to be wider on WF2 than it is on WF4 and WF3. This suggests the RC on WF2 has a larger contribution by comparatively young RC stars than the RC on WF3 and WF4. We selected stars on the [(F439W-F555W)$_0$, F555W$_0$] CMDs with $1.2 <$ (F439W-F555W)$_0 < 1.6$ and $23 <$ F814W$_0 < 24.5$. The

starcounts in the RC are characterized by the following mean F814W$_0$, sigma, and kurtosis: on WF2 23.89, 0.30, 0.09; on WF4 23.93, 0.25, 0.42; and on WF3 23.98, 0.24, -0.23.

Fig. 6 is a V, I CMD of all stars on all chips, which allows for a comparison with the V, I CMDs of Tolstoy et al. (e.g., their Figs. 6 and 16). Changes in the young stellar component with radius are readily apparent. In the Tolstoy et al. CMD of the center field of Leo A, the top of the MS is seen at an I magnitude of about 23. This compares to an I magnitude of about 24 in our data. The MS on the combined CMD is dominated by that of WF2, on WF3 and WF4 the top of the blue plume is clearly fainter yet. Star formation stopped at an earlier time in our outlying field, compared to the center, where it was active more recently. All of the Tolstoy et al. [V-I, I] WF chip CMDs show a prominent spur of BL stars emanating from the top of the RC. In our data, the BL stars are rather weak. They are prominent only on the WF2, weaker on the WF4, and very rare on the WF3 CMD. Interestingly both our V, I CMD and the CMD of Tolstoy et al. contain very few luminous red stars which could be interpreted as RSG or bright AGB stars. Tolstoy et al. barely detected the RC in their [B-V, V] CMD. In their V, I CMD, on the other hand, the RC is a strong, vertically extended feature, elongated along the magnitude direction. In our V, I CMD, the RC has a component that extends horizontally, along the color axis. This is the signature of a much older RC (see Caputo et al. 1995). We interpret this to indicate that old RHB stars become more obvious with increasing distance from the center of Leo A because the contribution of intermediate-age RC stars decreases as the mean population age increases.

Tolstoy et al. could not clearly distinguish HB stars in their V, I, or B, V CMDs, owing to the shallow limiting magnitudes which they were able to achieve. While we can distinguish RHB stars on our deeper CMDs, discriminating BHB stars against the MS component, which remains strong even at the position of our pointing, is not possible. We

place limits on a possible BHB component later in this paper.

In summary, the positional variations in the MS and BL stars as well as the changes in RC morphology and the detection of RHB stars, imply that the mean age of the stellar content of Leo A becomes greater with increasing distance from the center.

3. Results and Discussion

In general, the quantitative analysis of CMDs in terms of SFH is conducted by comparing the data with theoretical isochrones, tracks, or synthetic CMDs based on models of stellar evolution and atmospheres. This requires knowledge of the distance. Distance turned out to be an important parameter when Tolstoy et al. attempted to deduce the SFH at the center of Leo A. This problem remains acute in the interpretation of our data, as we attempt to find a solution which accommodates the magnitude of the TRGB, the color of the RGB and the location of the RHB stars.

3.1. Distance

In this section, we derive the distance to Leo A using the I-band TRGB. We use this distance to conduct the comparison with theoretical models which follows in the next sections. We also discuss the distance on pre- and post-Hipparcos distance scales. We emphasize that while the specific ages in the next section depend on our adopted distance scale, our main conclusions do not.

Table 3 of Tolstoy et al. (1998) is a summary of distances to Leo A derived with different methods and assumptions. There exists a wide range of distance moduli, from 23.9($\pm$0.1) to 24.9($\pm$0.7). In principle, our observations of Leo A offer two means for

deriving its distance, namely the TRGB and the RC.

A well-defined TRGB is present in >1 Gyr old stellar populations of a wide range of metallicities, and the absolute I-magnitude of the TRGB can yield a distance with a precision and accuracy similar to that of the Cepheid method (Lee, Freedman, & Madore 1993). A small metallicity correction may be applied; and a metallicity determination can be made from the V-I color of the RGB at either 0.5 or 1.0 mag below the TRGB (see Lee et al. 1993, also Bellazini, Ferraro & Pancino 2001). As long as the metallicity is lower than [Fe/H]≈-0.7, the TRGB in the I band is observed to be a constant to better than 0.1 mag. The location of the TRGB is commonly found by detecting a sharp edge in the I-band luminosity function of the red plume based on a [(V-I), I] CMD. In Fig. 6, we show the [$(V-I)_0$, I_0] CMD of our WFPC2 data. It is immediately obvious that the small number of stars detected in our field of view prohibits a reliable determination of the TRGB magnitude, or of the V-I color near the TRGB. We show in Fig. 6 that our CMD and our I-band LF are consistent with $I_{TRGB,0} = 20.5$, which is the value that Tolstoy et al. derived using ground-based, wide-field imaging. Tolstoy et al. did not trust the TRGB as a distance indicator because their data are consistent with a predominantly young stellar population. Our data, on the other hand, demonstrate that stars with ages of at least 9 Gyr are present in Leo A. We can ascertain that the data meet both the requirements, of a low metallicity *and* of a large age, which need to be satisfied before using the TRGB as a standard candle. The field of view of the ground-based images on which Tolstoy et al. based the TRGB is 9' x 9', overlapping both their, as well as our pointing. This justifies our adoption of the Tolstoy et al. ground-based TRGB.

In Fig. 7, we overplot the GC ridgelines of Da Costa & Armandroff (1990) onto our best V, I data, assuming $I_{TRGB,0} = 20.5$ and hence, $(m-M)_0$≈24.5, for Leo A. As can be seen from Fig. 7, the metallicity of the RGB stars of Leo A is near that of M 15, which has

[Fe/H]=-2.17. There are stars in Leo A which lie to the blue of M 15 GC ridgeline. Tolstoy et al. argued in part from this fact that the distance modulus of Leo A must be shorter than that indicated by the TRGB. However, there is a range of other explanations for these stars. They could be RGB stars with a metallicity below that of M 15. Some could be from the old AGB. And, since Leo A has formed stars over an extended period of time, we cannot exclude a young AGB or RGB, either. Tolstoy et al. do not provide an error for their ground-based TRGB value, but judging from the data, it appears that the error could be 0.1 – 0.2 mag. Adopting a dispersion for the metal-poor GC TRGBs of about ±0.05 (ignoring NGC 6397), the TRGB distance modulus of 24.5 for Leo A has an error of about ± 0.1 – 0.2 mag.

The GC ridgelines of Da Costa & Armandroff are on the "old" RR Lyrae distance scale which results from theoretical HB models of Lee, Demarque & Zinn (1990). This distance scale changed in the post-Hipparcos era, but it is not entirely clear what the new zeropoint is and how it depends on metallicity (e.g. Popowski & Gould 1999, Carretta et al. 2000). If we assume the calibration of Udalski (2000a), which corrects the TRGB to the RR Lyrae calibration of Popowski & Gould (1999), then M_I=-3.91(±0.05) for [Fe/H]<-0.7. The distance modulus of Leo A on this "new" RR Lyrae distance scale is $(m\text{-}M)_0$=24.4. The error is the same as that derived above, about ± 0.1 – 0.2 mag. We note that adopting this distance modulus for Leo A does not change the conclusion that its RGB stars are extremely metal poor.

The average RC magnitude has been calibrated empirically as a distance indicator. A discussion of its application to nearby galaxies may be found in Udalski (2000 a,b). RC stars occupy some of the same space as RGB/AGB stars on CMDs. In order to find $I_{RC,0}$, these components are usually separated by fitting the I-band luminosity function with two functions. We use a linear one for the RGB/AGB contribution, and a Gaussian one for

the RC contribution. In Fig. 8, we show the red plume LF based on our best V, I data, with such a fit overlayed. The color selection criterion is $0.5 \leq (V\text{-}I)_0 \leq 1.0$. From our fit we find the position of the RC, $I_{RC,0} = 24.05 \pm 0.05$, and its 1σ width, 0.20 ± 0.05. If we assume $M_I = (0.14 \pm 0.04)$ x ([Fe/H]+0.5) - 0.29 ± 0.05 from Udalski (2000a) and use [Fe/H]=-2.17 for the RC stars of Leo A, then M_I is -0.52 and the distance modulus for Leo A is $(m\text{-}M)_0 \approx 24.6$. Since we have neither determined a good value for [Fe/H] from our data, nor derived an [Fe/H] error, we can only give a lower limit to the distance modulus error from the RC method, >0.1 mag. The distance modulus from the RC method is consistent with that derived via the TRGB method.

Udalski worked on the assumption that the absolute I magnitude of the RC has a small dependence on metallicity, and virtually none on age, for 2—10 Gyr. This contrasts with theoretical work that suggests the absolute magnitude of the clump is a function of both age and metallicity (Girardi & Salaris 2001). Galaxies with ongoing star formation in particular, are found to exhibit an age distribution of clump stars which is strongly biased toward younger (1—3 Gyr) ages, and the RC magnitude gives a false distance if this is ignored.

Tolstoy et al. measured the RC at a mean I_0 magnitude of 23.73 (corrected for $A_I = 0.04$). This is 0.32 mag brighter than the RC we find in our data. Tolstoy et al. indicate that in their determination they favored the peak of the I histogram and its low-luminosity side over the high-luminosity side which they thought was obviously contaminated by BL stars. We also favored the peak in Fig. 8. Measurement errors or incompleteness, and calibration uncertainties, could easily account for about 0.1 mag, but are unlikely to be as large as several tenths of a magnitude. Assuming therefore that this difference is real, an alternative explanation could be age (and metallicity) biasing following Girardi & Salaris (2001). For example, if there is a lot of power in the young RC, it can easily bias the RC of

a composite stellar population toward a bright absolute I magnitude. As further support of this interpretation, we note that the weaker, secondary peak seen in Fig. 8 can be described by a Gaussian with a peak I_0 magnitude of 23.65±0.05 and a width of 0.15±0.05. This agrees with the peak RC magnitude found by Tolstoy et al.(1998). The differences in RC magnitude between the Tolstoy et al. data and our data could therefore be accounted for by the difference in pointing: the field of Tolstoy et al. was more centrally located and contains a population with a younger mean age than our outlying field, biasing their RC to a brighter magnitude.

As an aside we note that the age and metallicity dependence of the RC is still hotly debated between observers and theorists (e.g. Udalski 2000b). Leo A, with its extremely metal-poor stellar content and core-halo population gradient, may serve as a good future test case because theory predicts that the slope of $M_{RC,I}$ steepens with decreasing metallicity (Girardi & Salaris).

In summary, the application of both the TRGB and RC methods to our WFPC2 data consistently indicates that the distance to Leo A is m-M=24.5(±≈0.2)[3]. This value is larger than, but not inconsistent with, that of Tolstoy et al. (1998), who chose to adopt m-M=24.2(±0.2).

[3]Dolphin et al. (2002) derived a distance to Leo A based on their discovery of RR Lyrae variables with a mean V magnitude of 25.10±0.09. Using the calibration of Carretta et al. (2000), and adopting [Fe/H] = -1.7±0.3, they determine a true distance modulus of 24.51±0.12 for Leo A.

3.2. Comparison with Isochrones

Several databases for isochrones exist, but not all cover the metallicities and stellar phases which we need to interpret the Leo A data. The stellar-evolution models are based on different input physics, and different stellar atmospheres are adopted to convert from the theoretical to the observational plane.

We match the isochrones to the data by first determining the average I magnitude at the TRGBs of the oldest isochrones ($\geq$10 Gyr) in each database. We then shift the isochrones by the difference between the observed apparent TRGB magnitude and the theoretical absolute TRGB magnitudes in the I band. We adopt the following absolute I magnitudes at the TRGBs for the isochrones: for "old" Padua (i.e., Bertelli et al. 1994) Z=0.0004 (or [Fe/H]=-1.74), M_I=-4.1, m-M=24.6; for "new" Padua (Girardi et al. 2000, and http://pleiadi.pd.astro.it/) Z=0.0004, M_I=-4.0, m-M=24.5; Z=0.0001 (or [Fe/H]=-2.36), M_I=-3.9, m-M=24.4; for Yale (Yi et al. 2001) Z=0.0004, M_I=-4.1, m-M=24.6; Z=0.0001, M_I=-4.0, m-M=24.5; and for Frascati (Cassisi, Castellani & Castellani 1997) Z=0.0001, M_I=-4.1, m-M=24.6. We note that all of the isochrones have I-band TRGBs which yield distances that are consistent with our empirical distance estimate. We also note that the isochrones predict the location of the RC at different magnitudes; this is illustrated to some extent by the figures in this section (also see Castellani et al. 2000, for a detailed discussion).

Tolstoy et al. (1998) modeled their Leo A data with the old Padua models. The Z=0.0004 isochrones provided a good description of the young stellar content. This is not surprising, because their metallicity is similar to the oxygen abundance of the ionized ISM of Leo A. Since the work of Tolstoy et al., a new set of Padua isochrones was published. We therefore provide in Fig. 9 a comparison of our data with both the old and the new Padua isochrones. As can be seen from Fig. 9, the difference between the old and the new Padua

isochrones is rather small.

We show three sets of isochrones which represent the young, intermediate-age, and old stellar content of Leo A. The densely populated area of the blue plume can be interpreted to contain young MS stars. The MSTO of a 200 Myr isochrone matches well the top of the MS, while the detection limits in the blue plume correspond to the MSTO of about the 2 Gyr isochrone. The less densely populated part of the blue plume above $I_0 \approx 24$ can be accounted for with BSG and BL stars with ages of about 200 Myr and older. The few bright stars located between the blue and red plumes can similarly be ascribed to BL stars with ages of a few hundred Myr. Stars just blueward of the top of the RC are consistent with stars less than about 500 Myr old which are in the core-He burning phase. While the isochrones extend well above the TRGB, they predict a very small number of luminous red stars, as observed. The bottom of the densely populated area of the blue plume might contain BHB stars with ages well in excess of 10 Gyr. The 18 Gyr isochrone suggestively connects the RHB stars to a handful of stars at $I_0 \approx 25$ just redward of the blue plume. Alternatively, these stars could be just beyond the MSTO of a young, $\approx$1 Gyr population. The 18 Gyr isochrone extends only slightly above the TRGB to include AGB stars. Indeed, few stars are observed here.

The RC area is characteristic of an intermediate-age population. The 2 Gyr isochrone is shown to illustrate the upper age limit derived by Tolstoy et al. from their centrally-located field. Indeed the bright, red portion of the RC can be associated with ages of around 2 Gyr in our data as well. But a substantial number of stars with ages above 2 Gyr is required to match the entire extent of the RC, and in particular, its faint, blue portion. The 2 Gyr isochrone remains blueward of the RGB in both CMDs (and so would a Z=0.0001, 2 Gyr Padua isochrone).

Therefore, in order to explain the RGB stars of Leo A with isochrones of metallicity

Z=0.0004, old ages are required, but even they cannot provide a perfect match. The 18 Gyr isochrone shown in Fig. 9 stays slightly blueward of the TRGB in the [(V-I)$_0$, I$_0$] CMD, and is slightly red for portions of the [(B-I)$_0$, I$_0$] RGB of Leo A. The fact that the RGB can be explained with ancient stars of such a high metallicity contradicts our results from using GC ridgelines. The empirical GC ridgelines indicate both old *and* very metal-poor stars. Indeed, it is well known that, being very sensitive to the stellar atmospheres adopted, the slopes of theoretical giant branches are difficult to predict in the observational plane.

In Fig. 10, we overplot onto our [(B-I)$_0$, I$_0$] CMD Yale isochrones of intermediate and old ages for Z=0.0004, and Z=0.0001. For Z=0.0004, a predominantely intermediate-age RGB provides the best match to the data. For Z=0.0001 (slightly lower than the metallicity of the M 15 RGB), on the other hand, even the oldest isochrones are to the blue of the observed RGB. These isochrones suggest that for metallicities $Z \leq 0.0004$, there are RGB stars with a minimum age of 5 Gyr.

The Padua and the Frascati databases include the HB phase. In Fig. 11, we overplot the Leo A [(B-I)$_0$, I$_0$] CMD with intermediate-age and old isochrones from these databases. We show Padua isochrones for Z=0.0004 which we know can fit the RGB/AGB; but this time our goal is to investigate the RC/RHB. We find that they are slightly too faint at the RC/RHB. We also show Padua and Frascati isochrones for Z=0.0001. The Padua Z=0.0001 isochrones are too blue on the RGB; however, because they are bright in the core-He burning phase, they can give a good characterization of the RC/RHB. The 5 Gyr isochrone, for instance, is a good match to the RC stars. The 10 Gyr isochrone extends slightly blueward of the data, indicating that the blue edge of the RHB is just under 10 Gyr of age. The Frascati Z=0.0001 isochrones match very well the RGB/AGB stars of Leo A, and suggest a population which is predominantly several Gyr old. At the same time, the bluest RC/RHB stars can be accounted for with the 5 and 10 Gyr isochrones, while the

14 Gyr isochrone extends beyond the blue edge of the RHB in the data. Since the location of HB stars also depends on how much mass loss is assumed on the RGB, we cannot give a firm age limit based on the blueward extension of the RHB.

We summarize our findings as follows. Stars with a wide range of ages, between about 0.2 and 2 Gyr, make up the young stellar content of Leo A within our field of view. Stars of such young ages cannot account for the location of the RGB and the RC in the data. A minimum age of about 5 Gyr is required for metallicities between Z=0.0004 and 0.0001 in order to explain the color of the RGB/AGB in Leo A. For similar metallicites, the bulk of the RC stars is several Gyr old. The blueward extent of the RHB is consistent with ages of up to about 10 Gyr.

3.3. Comparison with Synthetic CMDs

The RHB overlaps partially with the RC and RGB/AGB, while the BHB coincides largely with MS stars. In order to investigate how much of a horizontal branch component is consistent with our CMDs of the outer regions of Leo A, we here present synthetic CMDs of the stellar content in the WF3 & WF4 chips.

Synthetic CMDs, which are based on theoretical stellar evolutionary tracks and atmospheres convolved with the photometric errors and completeness fractions of the data, can provide a more complete picture of the SFH than is possible with the isochrone comparison conducted in the previous section. Here, we use the Bologna Code (Greggio et al. 1998) with the Padua tracks of metallicity Z=0.0004 (Fagotto et al. 1994), the same ones adopted by Tolstoy et al. (1998), and the stellar atmospheres of Bessel, Castelli & Plez (1998). The data errors and the recovery fractions from false star tests on WF3 & WF4 are shown in Figs. 3 & 4. We incorporated photometric uncertainties and completeness

fractions based on these results into the simulator. For reference, the distance modulus implied by the tracks is 24.6; at this distance, the area of the two WF chips equals 0.19 kpc^2, and absolute model SFRs may be transformed into SFRs/area accordingly.

It should be noted that the completeness tests were carried out in coarse bins; and this provides a limitation to the comparison of the models and the data in the faintest magnitude bin near the completeness limits. Furthermore, as shown by Fig. 3, there are a few outlying V and I errors compared with the broad band which defines most of the errors. The simulator was programmed to contain the broad band of errors; but we did not attempt to include the outliers. Therefore, we anticipate mismatches of the model with the data for the faintest magnitude bin, and we expect the synthetic CMDs to lack a smattering of objects with extreme colors. There are additional sources of error which are not included in the simulations. Internal, differential reddening does not appear to be important in Leo A, and was neglected. Contamination by foreground stars also is a very small source of error which we did not address with the simulations.

The simulations presented here assume a Salpeter (1955) initial mass function (IMF) with the standard slope of 2.35. Since many investigations of the SFRs and SFHs of dIrr galaxies have assumed mass limits from 0.1 to 100 $M_\odot$, we do so as well. The primary constraint of the modeling is that any linear combination of synthetic star forming events has to produce 1738 surviving stars on the CMD with colors and luminosities which are in broad agreement with the data. We followed the same methodoloy as Schulte-Ladbeck et al. (2000, 2001) and Crone et al. (2002), in that we started by identifying boxes in color and magnitude which contain stars with progressively older ages. We then modeled the stars in each box with a constant SFR. For example, an appropriate constraint of the recent SFH within the past few hundred Myrs can be obtained by considering the BL descendants found at colors of about $-0.4 < (V\text{-}I)_0 < 0.4$ and $22 < I_0 < 23.5$. The number of stars

observed between about $0 < (V\text{-}I)_0 < 0.4$ and $24 < I_0 < 25.5$ can be used to constrain the BHB stars, for which the isochrones have indicated extremely large ages. The bulk of the stars seen on the CMD is in the RC.

Whenever we model the SFH of a galaxy, we first ask whether there are any features that force us to assume a variable SFR over time. Therefore, in Fig. 12, we first show a model with a constant SFR from 12 Gyr ago until the present. We then present two types of models with variable SFRs with time which are rooted in two distinct hypotheses. The basic assumption of Model 1 (Fig. 13a) is that there are no BHB stars in Leo A. This is the model which will be most readily comparable with the result of Tolstoy et al. (1998). Model 2 (Fig 13b) investigates how much of an ancient BHB can be hidden in the data, and was designed to contain the maximum number of BHB stars allowable by the data.

We start by describing the fiducial model with 12 Gyr, constant SFR shown in Fig. 12. For reference, such a model has a SFR of about 3.17 to 3.36 x 10^{-5} $M_{\odot}yr^{-1}$. In the region I<24, -1.0<(V-I)<0.5, this model produces more MS stars than the data, and has a distinct BL which the data lack as well. There are very few stars involved in producing the upper MS and these BL stars, hence we are limited by small-number statistics. On the other hand, it is easy enough to dis-allow very recent SF (so that the top of the MS becomes fainter), and to reduce the SFR which gives rise to the bluest BL stars. In the region I<24,(V-I)>0.5, the model does quite well in producing the correct number of stars in the upper RGB, and it is also successful in providing the observed number of stars in the RC as well as the mean RC brightness. There is a spur of BL stars near (V-I)≈0.6, which connects to the top of the RC. Dis-allowing SF with ages near 1 Gyr avoids this "blue finger" morphology. In the region 26>I>24, -1.0<(V-I)<0.5 the model produces significantly too many stars in the blue plume. There is no indication of the blue stars between the RC and the MS, which we could interpret as BHB stars. However, the number of stars observed here is small, so this

difference could be attributed to statistics. In the region (V-I)>0.5, there are significantly too few red, RGB stars below the RC. We therefore find that we cannot achieve a good match of the data with a model that assumes constant star formation over the past 12 Gyr, and must look to a time-variable SFR.

Next, we take inspiration from Tolstoy et al., who found that they needed to produce at least 60% of the stars on their CMD in a short burst of star formation with ages from 0.9 to 1.5 Gyr. In Fig. 12, we illustrate the effect of such a SFH in our data. It generates a completely different RC morphology from the one we observe. The RC is round, not tilted; its mean brightness is too high. Furthermore, the upper RGB is blue and quite narrow. (The same morphology appears when we assume the Tolstoy et al. distance modulus, but the RC becomes even brighter and the upper RGB, even bluer). There are very few stars on the RGB below the RC, where our data show a significant component. Therefore, a better model SFH requires ages which reproduce correctly the mean location of the RC, and also populates the lower part of the RGB/AGB without overpopulating its upper part above the RC. The model discussed here also serves to indicate that the spur of stars which we believe to be the signpost of a potential BHB component cannot be interpreted as the SGB of a burst of star formation that occured about 1.1 Gyr ago. This would bring along too many stars in the top blue part of the RC. We conclude that we demonstrated with the help of synthetic CMDs our earlier inference that the SFH in the outer regions has clearly been different from that in the inner regions of Leo A.

A solution for our "no BHB" hypothesis is shown in Fig. 13a, top right. We first describe qualitatively, the ingredients and constraints which went into this model. We did not produce any very young stars in order to avoid making stars which are too luminous compared with the data, but we provide an upper limit below. Any SFH which would produce most of the stars in the blue plume with a young stellar component brought along

too many BL stars. Therefore, we introduced a gap in the SFH at around 1 Gyr and looked to the intermediate-age population to provide additional stars for the bottom of the blue plume. Any model that produced the required number of RC stars also brought along RGB/AGB stars, as well as SGB stars which populate the bottom of the blue plume. Therefore, there is some crosstalk between the intermediate-age and the recent SF. A synthetic RC aged 2—3 Gyr populated the bottom of the blue plume very well, but the mean luminosity of the RC was still too bright compared with the data (see Fig. 12). We also could not produce an RC with a simple, continuous SFR from 2—10 Gyr, and at the same time, provide a sufficient amount of stars to fill in the bottom of the CMD (see Fig. 12).

Our best "no BHB" model is qualitatively rather similar to that of Tolstoy et al. (1998). We first tried to produce as young an RC as the data would allow. This yielded an ample amount of SGB stars in the bottom of the blue plume, and we re-iterated on the SFH that produced the upper part of the blue plume accordingly. In this fashion we successfully synthesized an appropriate number of BL stars, and an acceptable luminosity function for the blue plume. The young RC solution, however, fell short of synthetic stars in the the bottom half of the RC, of RHB stars, and of stars on the RGB/AGB. These stars were provided in the next step. Adding this third component allowed us to accomplish several things. We found that it was possible to make these stars old enough to avoid significant crosstalk with the blue plume, while bringing along enough stars in the bottom part of the RC, and in the RHB. Also, this component provided stars on the RGB/AGB, which, in the region above the RC, have red colors. This improved how well the model reproduces the overall appearance of the RGB/AGB.

Fig. 13a, bottom, illustrates what kind of Model 1 SFHs are compatible with the data. There is no star formation in the recent 0.15 Gyr. As stated before, we suffer from small

number statistics here. We could easily allow a SFR of 5 x 10^{-6} $M_{\odot}yr^{-1}$ in recent times. The model has a young component with ages between 0.15 and 0.8 Gyr which has a SFR between 3.13 and 3.87 x 10^{-5} $M_{\odot}yr^{-1}$, an intermediate-age component with an age range from 1.7 to 4.5 Gyr with a SFR of 6.22 to 7.67 x 10^{-5} $M_{\odot}yr^{-1}$, and an old component with ages from 10 to 14 Gyr for which the SFR is between 5.98 to 6.41 x 10^{-5} $M_{\odot}yr^{-1}$. Although the SFR during the age interval 0.8 – 1.7 Gyr is zero for the example in Fig. 13a, we cannot rule out star formation at the level of a few times 10^{-6} $M_{\odot}yr^{-1}$ during this interval. By pushing part of the RC to young ages, and part of the RC to old ages, we produced a third gap in the SFH. It is quite likely that the gap is not real. Instead of two epochs of SF separated by a zero SFR from 4.5 to 10 Gyr, slow modulations in the intermediate and old SFR could produce similar CMDs. The possible parameter space for solutions is large, and we did not explore it exhaustively. Stars with a wide range of masses and hence ages overlap in the area of the CMD which encompasses the RC; this introduces considerable degeneracy.

We again find that the models suggest stars in more outlying regions of Leo A have higher mean ages. The young RC in the outer regions has an age of about 3 Gyr, compared to 1.2 Gyr in the inner regions (Tolstoy et al.). In Model 1, about 30% of the synthetic stars on the CMD are in the ancient component. In terms of the astrated mass, the ancient stars of Model 1 account for 1.14 times that in young and intermediate-age stars.

Fig. 13b, top right, shows a solution for the "maximum BHB" hypothesis. There are considerable degeneracies in the model. Any event that produces BHB stars populates the middle and bottom part of the blue plume, and thus interferes with the young stellar component here, as well as with intermediate-age SF that populates SGBs near the bottom of the blue plume. We therefore started this model with the box that contains the BHB stars. Being our "maximum BHB" model, we tried to account for as many blue plume stars

as possible with this component. This event also brought along a population of RHB stars and RGB/AGB stars. By adjusting the duration of the SF event, we could find a pleasing morphology for the HB. It was much simpler than in Model 1, to then also find a good solution for the RC, since the RHB stars at the bottom of the RC, and some RGB/AGB stars were already accounted for. It was also easier with Model 2, to fill in the rest of the blue plume without overproducing BL stars. As intended, Model 2 yields copious stars with I $\approx$ 25 between the two plumes where Model 1 shows none.

Model 2 has a young component with ages from 0.05 to 0.55 Gyr and SFRs between 2.85 and 3.07 x 10^{-5} $M_{\odot}yr^{-1}$, an intermediate-age component aged 1.5 to 7.5 Gyr and with SFRs in the range from 4.63 to 5.06 x 10^{-5} $M_{\odot}yr^{-1}$, plus an ancient stellar content with ages from 19.5 to 24 Gyr and SFRs between 5.92 to 6.67 x 10^{-5} $M_{\odot}yr^{-1}$. In comparison with the inner regions of Leo A as modeled by Tolstoy et al., Model 2 suggests a much higher mean age, of about 5.25 Gyr, for the bulk of the stars seen on the CMD of the outer regions. The ancient population of Model 2 accounts for 20% of the stars on the CMD, and its mass is 0.93 times that in young and intermediate-age stars.

As was anticipated from the isochrone comparison in the previous section, the assumption of the presence of BHB stars requires very low-mass stars, which go along with very high ages in our database. Specifically, the ages needed to produce a significant BHB are well in excess of the age of the Universe. There is an alternative interpretation, which would make our Model 2 a more viable solution, and that is to allow for more mass loss on the RGB (see Lee, Demarque & Zinn 1994). Our models assumed Reimer's (1975) formula with η=0.3 (the canonical parameter calibrated on the average properties of Galactic halo GCs). In this way, a star loses about 0.1 $M_{\odot}$ on the RGB. If stars lose mass more efficiently on the RGB before they populate the HB, then low HB masses map onto younger ages. For example, re-scaling the ages of the stars which populate the BHB in our models for a mass

loss of 0.2 $M_{\odot}$, shows their median age drops from 21.7 Gyr, to 11 Gyr! The apparent gap in SFR between 7.5 and 19.5 Gyr may therefore be considered an artifact of the RGB mass loss we choose; an increased mass loss on the RGB would allow for a younger absolute age of the onset of SF, as well as for a different modulation from that of Model 2, in the SFR at intermediate and old ages.

In summary, we find that the SFR in the outer regions of Leo A has been very low in the most recent times, <0.1 Gyr ago, and was also very small around about 1 Gyr ago. We cannot produce a synthetic CMD which matches the data if the bulk of the stars is between 0.9—1.5 Gyr old. We also cannot successfully model the data without allowing any stars with ages well beyond 2 Gyr. As was clear from the isochrones, the presence of a RHB demands stars with comparatively old ages. Just how old these stars are cannot be determined. In Model 1, we produced a relatively young, 3 Gyr luminous RC, and combined it with a 12 Gyr RC/RHB. In Model 2, we used a 5.25 Gyr RC and combined it with a 21.75 Gyr HB. Both models yield acceptable solutions in terms of CMD morphologies and luminosity functions. Both models indicate an overall declining SFR from early times to today.

The exploration of the SFH of Leo A with synthetic CMDs based on the Z=0.0004 old Padua stellar evolution database has allowed us to gain additional insights into the temporal and spatial dependence of the SFR in Leo A. A more complete study of the SFH of Leo A, using both the dataset of Tolstoy et al. (1998) as well as our data, and analyzed with the same techniques and assuming the same distance modulus, is desirable, but beyond the scope of the present work. In particular, Castellani et al. (2000) present arguments that the new Padua tracks by Girardi et al. are preferred to simulate the RC. But Tolstoy et al. (1998) used the old Padua models, and so did we for the simulations presented in this paper. We also did not explore any metallicity evolution with the present simulations.

If ongoing SF enriched the ISM of Leo A, then metallicity changes with time are a likely candidate for widening the V-I color of the RGB/AGB. Here, its width was produced with age differences, only. Conceivably, the stars on the BHB could belong to a different SF episode than the RHB stars; if metallicity evolution is important the BHB stars could also have different metallicites from those on the RHB. The model-SFH of Leo A and its total astrated mass depend sensitively on how much mass loss is assumed on the RGB.

The simulations verify the results of the isochrone comparison by indicating that Leo A is an unlikely candiate for a delayed-forming dwarf galaxy. The intriguing possibility of the detection of a BHB should encourage deeper observations at larger galactocentric radii covering a wider field of view. The measurement of ancient MSTOs, in particular, is needed to unambiguously confirm the existence of a history of early star formation.

4. Conclusions & Implications

We present deep B, V, & I single-star photometry of an off-center WFPC2 field in Leo A, and use CMDs to discover the presence of metal-poor RHB stars. From this detection alone we can conclude that Leo A contains some stars which have ages similar to the equivalent stars in Galactic GCs. Finding stars with old ages validates the use of the TRGB as a distance indicator to Leo A. There is a significant component of young stars in our field, especially on the WF2 chip, and to a lesser degree, on the WF3 & WF4 chips as well. We cannot discriminate BHB stars from this young stellar content, but present synthetic CMDs of WF3 & WF4, which indicate the presence of BHB stars is possible.

How old are the RHB stars which we see? The absolute ages of GCs depend on their distances, but the relative ages of metal-poor GCs which contain a RHB can be interpreted to indicate that they could be about 1—2 Gyr younger than the oldest GCs (e.g. Lee et al.

2001). Assuming that the oldest clusters are between 11 and 13 Gyr old (Reid 1999), then a reasonable lowest age limit for GCs with a metal-poor RHB is 9 Gyr. Therefore, Leo A, showing a RHB and a metal-poor population, is at least 9 Gyr old.

We find that with a distance modulus of 24.5±0.2 on a short RR Lyrae distance scale, we can simultaneously account for the I-band magnitude of the TRGB in ground-based data, and for the mean I-band magnitude of the RC in our WFPC2 field. A comparison with GC ridgelines indicates that the RGB has [Fe/H] smaller than 1% of Solar, which is below the O abundance of the ionized ISM, 3% of Solar. Theoretical isochrones from a wide range of databases can account for the locations in color and magnitude of the RGB/AGB branches, and of the RC/RHB of Leo A, when the stellar metallicities are assumed to be between $0.0001<Z<0.0004$ (0.5-2% of Solar) and the stellar ages are between 5 and 10 Gyr.

We use synthetic CMDs to evaluate the mean age of the RC stars. In the CMD of the inner regions as modeled by Tolstoy et al. (1998), the RC has a mean age of about 1.2 Gyr. The bulk of the stars which populate the RC on the CMD of the outer regions is 3 Gyr old in our Model 1, and 5.25 Gyr old in our Model 2. Additionally, about half of the astrated mass of either set of models resides in an ancient stellar population. The exact age of this population can be adjusted depending on just how much mass loss is allowed on the RGB. The synthetic CMDs thus suggest a stellar substratum/halo population older than 9 Gyr is not inconsistent with the data, but its confirmation requires future deep, wide-field imaging further out in the halo of Leo A.

Our findings have a variety of implications. Leo A joins the ranks of other star-forming dwarf galaxies which show a population gradient. While the mean age of the central regions of Leo A is predominantly young, the mean age progressively increases with increasing galactocentric distance. The youngest MS, BSG, and BL stars are more concentrated toward the center; their numbers fall off more rapidly with distance than those of the RGB

stars which are present throughout the entire galaxy.

Leo A is not a young galaxy in the sense that it has not made its very first stars in the past 2 Gyr. Our data clearly show the signatures of old, metal-poor stars. The cosmic SFR density has a peak at a redshift of z≈1.5 (e.g. Boselli et al. 2001, Fig. 8, Hopkins et al. 2001, Fig. 1). Depending on the cosmological model, this redshift corresponds to lookback times of about 6.5—8.5 Gyr (see Hopkins et al., Figs. 3 and 4). Our limiting age of >9 Gyr for the oldest stars detected, indicates that the first stars in Leo A were in place before the cosmic SFR density started to decline. Our findings therefore add to the increasing evidence that some stars formed early on, 9 Gyr ago or earlier, in a wide range of Local Group galaxies.

We see in Leo A an extended history of star formation spanning billions of years. As with many other local dwarfs with deep CMDs, Leo A cannot readily be identified as a delayed-formation dwarf. The delayed-formation-of-dwarfs-scenario blossomed when it seemed to be able to explain the excess of faint blue galaxies (e.g., Babul & Ferguson 1996). We have since learned that the highest SFRs observed in the fossil record of local dwarfs (which typically allow a detailed construction of their star formation history over the past $\sim$ Gyr) are rarely ever high enough to account for the blue luminosities required of such briefly bursting dwarfs, and that the time-scales for star formation are usually longer than the 10 Myr assumed in the Babul & Ferguson scenario (Greggio et al. 1998, Lynds et al. 1998, Schulte-Ladbeck et al. 2001, Tosi 2001). Therefore, such an extreme bursting mode seems unlikely. Furthermore, the direct observation of (potentially) high metallicities, i.e., oxygen abundances, in faint blue galaxies suggests that they are typically higher mass systems than local dwarfs (Carollo & Lilly 2001).

The discovery of a young galaxy in the local Universe would have profound implications for theories of galaxy formation, and this possibility has long motivated searches for galaxies

with very low oxygen abundances and very blue colors (Sargent & Searle 1970; Izotov & Thuan 1999; Kunth & Östlin 2000). The existence of old stars in Leo A, however, joins mounting evidence that star-forming dwarf galaxies in the local Universe do contain old stars, no matter how low the metallicity of their ionized gas. In other words, an extremely low oxygen abundance does not imply a recently formed galaxy.

We thank Dr. E. Tolstoy for supplying us with her photometry of the inner regions of Leo A. We are grateful to Claus Gössel for obtaining the R-band image of Leo A at the Wendelstein Observatory of the University of Munich. We would also like to thank Dr. C. Maraston for sharing with us her set of Frascati isochrones. We made extensive use of the SIMBAD and NED databases. This work was supported by an HST grant associated with GO program 8575. UH would also like to acknowledge financial support from SFB 375.

REFERENCES

Aloisi, A., Tosi, M., Greggio, L. 1999, AJ, 118, 302

Babul, A., Ferguson, H.C., 1996, ApJ, 458, 100

Barkana, R., Loeb, A. 2001, astro-ph/0010468, to be published in Physics Reports 2001

Ballazzini, M., Ferraro, F.R., Pancino, E. 2001, ApJ (astro-ph/0104114)

Bessel, M.S., Castelli, F., Plez, B. 1998, A&A, 1998, 337

Bertelli, G., Bressan, A., Chiosi, C., Fagotto, F., Nasi, F. 1994 A&AS, 106, 275

Boselli, A., Gavazzi, G., Donas, J., Scodeggio, M. 2001, AJ, 121, 753

Caputo, F., Castellani, V., Del'Innocenti, S. 1995, A&A, 304, 365

Carollo, C.M., Lilly, S.J. 2001, ApJ, 548, L153

Carretta, E. Gratton, R.G., Clementini, G., Fusi Pecci, F. 2000, ApJ, 533, 215

Castellani V., Degl'Innocenti, S., Girardi, L., Marconi, M., Prada Moroni, P. G., Weiss, A. 2000, A&A, 354, 150

Castelli F., Gratton, R.G, Kurucz, R.L. 1997a, A&A, 318, 841

Castelli F., Gratton, R.G, Kurucz, R.L. 1997b, A&A, 324, 432

Castelli F., Degl'Innocenti, S., Girardi, L., Marconi, M., Prada Moroni,P.G., Weiss, A. 2000, A&A, 354, 150

Cassisi S., Castellani, M., Castellani V. 1997, A&A 317,108 reference Cole, A.A., Tolstoy, E., Gallagher, J.S. et al. 1999, AJ, 118, 1657

Cotton, W.D., Condon, J.J., Arbizzani, E. 1999,ApJS, 125, 409

Crone, M.M., Schulte-Ladbeck, R.E., Greggio, L., Hopp, U. 2002, ApJ, 567, 258

Da Costa, G.S., Armandroff, T.E. 1990, AJ, 100, 162

Demers, S., Kibblewhite, E.J., Irwin, M.J., Bunclark, P.S., Bridgeland, M.T. 1994, AJ, 89, 1160

Dekel, A., Silk, J. 1986, ApJ, 303, 39

Dolphin, A.E., Saha, A., Skillman, E.D., Tolstoy, E., Cole, A.A., Dohm-Palmer, R.C., Gallagher, J.S., Mateo, M., Hoessel, J.G. 2001, ApJ, 550, 554

Dolphin, A.E., Saha, A., Claver, J., Skillman, E.D., Cole, A.A., Gallagher, J.S., Tolstoy, E., Dohm-Palmer, R.C., Mateo, M., 2002, AJ, in press, astro-ph/0202381

Duc, P.-A., Mirabel, I.F. 1998, A&A, 333, 813

Durrell, P.R., Harris, W.E. 1993, AJ, 105, 1420

Ellis, R.S. 1997, ARA&A, 35, 389

Fagotto, R., Bressan, A., Bertelli, G., Chiosi, C. 1994, A&AS, 105, 29

Ferrara, A., Tolstoy, E. 2000, MNRAS, 313, 291

Girardi, L., Bressan, A., Bertelli, G., Chiosi, C. 2000 A&AS, 141, 371

Girardi, L., Salaris, M. 2001, MNRAS, 323, 109

Greggio, L., Tosi, M., Clampin, M., De Marchi, G., Leitherer, C., Nota, A., Sirianni, M. 1998, ApJ, 504, 725

Grebel, E.K., 1999, in IAU Sump. 192, The stellar Contnet of the Local Group, eds. p. Whitelock & R. Cannon (Provo: ASP), 17

Grebel, E.K., 2000, astro-ph/0008249, to appear in "Microlensing 2000: A New Era of Microlensing Astrophysics", Cape Town, South Africa, ASP Conf. Ser., ed. J.W. Menzies and P.D. Sackett

Harbeck, S., Brebel, E.K., Holtzman, J., Guuhathakurta, P., Brandner, W., Geisler, D., Sarajedini, A., Dolphin, A., Hurley-Keller, D., Mateo, M. 2001, astro-ph/0109121

Hesser, J. E., Harris, W. E., Vandenberg, D. A. 1987, PASP, 99, 1148

Hodge, P.W., Dolphin, A.E., Smith, T.R., Mateo, M. 1999, ApJ, 521, 577

Holtzman J.A., Burrows C.J., Casertano S., Hester J.J., Trauger J.T., Watson A.M., Worthey G., 1995, PASP, 107, 1065

Hopkins, A.M., Irwin, M.J., Connolly, A.J. 2001, ApJ, 558, L31

Izotov, Y.I., Thuan, T.X. 1999, ApJ, 511, 639

Izotov, Y.I., Chaffee, F. H., Foltz, C.B., Green, R.F., Guseva, N.G., Thuan, T.X. 1999, ApJ, 527, 757

Klypin, A., Kravtsov, A.V., Valenzuela, O., Prada, F. 1999, ApJ, 522, 82

Kunth, D., Östlin, G. 2000, A&AR, 10, 1

Lee, M.G., Freedman, W.L., Madore, B.F. 1993, ApJ, 417, 553

Lee, Y.-W., Demarque, P., Zinn, R. 1990, ApJ, 350, 155

Lee, Y.-W., Demarque, P., Zinn, R. 1994, ApJ, 423, 248

Lee, Y.-W., Yoon, S.-J., Rey, S.-C. 2001, to appear in "Astrophysical Ages and Time Scales, ASP Conf. ser., edts. T. von Hippel, N. Manset, & C. Simpson, astro-ph/0104405

Lejeune, Th., Schaerer, D. 2001, A&A, 366, 538

Lynds, R., Tolstoy, E., O'Neill, E.J., Jr., Hunter, D.A. 1998, AJ, 116, 146

Marzke, R.O., Da Costa, L.N. 1997, AJ, 113, 185

Mateo, M. 1998, ARA&A, 36, 435

Mateo, M. 2000, in "The First Stars", Proceedings of the MPA/ESO Workshop held at Garching, Germany, 4-6 August 1999, Achim Weiss, Tom G. Abel, Vanessa Hill (eds.), Springer, p. 283

Mighell, K.J., Sarajedini, A., French, R.S. 1998, AJ, 116, 2395

Minniti, D., Zijlstra, A.A. 1996, ApJL, 467, 13

Östlin, G. 2000, ApJL, 535, 99

Origlia, L., Leitherer, C. 2000, AJ, 119, 2018

Popowski, P., Gould, A. 1998, in "Post-Hipparcos Cosmic Candels", A. Heck, F. Caputo (eds.), Kluwer Academic Publ., Dordrecht, p. 53

Reid, I.N. 1997, AJ, 114, 161

Reid, I.N. 1999, ARA&A, 37, 191

Reimers, D. 1975, in "Problems in Stellar Atmospheres and Envelopes", ed. B. Baschek, W. H. Kegel, & G. Traving (Berlin: Springer), 229

Rejkuba, M., Minniti, D., Gregg, M.D., Zijlstra, A.A., Alonso, M.V., Goudfrooij, P. 2000, AJ, 120, 801

Rood R.T. 1973, ApJ, 184, 815

Roukema, B.F., Peterson, B.A., Quinn, P.J., Rocca-Volmerange, B. 1997, MNRAS, 292, 835

Roukema, B.F. 1998, in "Dwarf Galaxies and Cosmology", Proceedings of the 33^{rd} Moriond Astrophysics Meeting held at Les Arcs, France, Narch 14-21, 1998, ed. T.X. Thuan, C. Balkowski, V. Cayrate, J. Tran Thanh Van, Editions Frontières, p. 471

Saha, A., Freedman, W.L., Hoessel, J.G., Mossman, A.E. 1992, AJ, 104, 1072

Salpeter, E.E. 1995, ApJ, 121, 161

Sandage, A. 1970, ApJ, 162, 842

Sargent, W.L.W., Searle, L. 1970, ApJL, 162, 155

Schulte-Ladbeck, R.E., Hopp, U., Crone, M.M., Greggio, L. 1999, ApJ, 525, 709

Schulte-Ladbeck, R.E., Hopp, U., M.M., Greggio, L., Crone, M.M. 2000, AJ, 120, 1713

Schulte-Ladbeck, R.E., Hopp, U., Greggio, L., Crone, M.M., Drozdovsky, I.O. 2001, AJ, 121, 3007

Silbermann, N.A., Smith, H.A. 1995, AJ, 110, 704

Skillman, E.D., Kennicutt, R.C., Hodge, P. 1989, ApJ, 347, 875

Stetson, P.B. 1994, PASP, 106, 250

Tolstoy, E., Gallagher, J.S., Cole, A.A., Hoessel, J.G., Saha, A., Dohm-Palmer, R.C., Skillman, E.D., Mateo, M., Hurledy-Keller, D. 1998, AJ, 116, 1244

Tosi, M. 2001, review paper to appear in 'Dwarf Galaxies and their Environment", K.S. de Boer, R.J. Dettmar, U. Klein eds. (Shaker Verlag, De), astro-ph/0104016

Tosi, M., Sabbi, E., Bellazzini, M., Aloisi, A., Greggio, L., Leitherer, C., & Montegriffo, P. 2001, AJ 122, 1271

Udalski A. 2000a, Acta Astron., 50, 279

Udalski A. 2000b, ApJ, 531, L25

Walker, A. 1989, PASP, 101, 570

White, S.D.M., Springel, V. 2000, in "The First Stars", Proceedings of the MPA/ESO Workshop held at Garching, Germany, 4-6 August 1999, ed. A. Weiss, T. G. Abel, V. Hill, Springer, p. 327

van Zee, L., Skillman, E.D., Haynes, M.P. 1999, AAS, 194.0504

Yi, S., Demarque, P., Kim, Y.-C., Lee, Y.-W., Ree, C., Lejeune, Th., Barnes, S. 2001, ApJ, in press (astro-ph/0104292)

Fig. 1.— The locations (WFPC2 footprints) of the Tolstoy et al. data (GO program 5915) and of our data (GO program 8575) relative to a Leo A R-band image obtained at the Wendelstein Observatory. The WFPC2 insets show the resolved stars in the V filter, and have been scaled relative to one another based on total exposure time. Two WF chips side-by-side have a length of 154"; this provides a sense of scale for this image.

Fig. 2.— a. The CMD of resolved stars in each of the WFPC2 chips for the first filter combination.

Fig. 2b. – The CMD of resolved stars in each of the WFPC2 chips for the second filter combination.

Fig. 2c. – The CMD of resolved stars in each of the WFPC2 chips for the third filter combination.

Fig. 3.— DAOPHOT photometric errors for all three filters on the WF3 and WF4 chips (magnitudes transformed to B, V, I).

Fig. 4.— Completeness tests from ADDSTAR for all three filters on the WF3 and WF4 chips (magnitudes transformed to B, V, I).

Fig. 5.— a. Luminosity functions along the blue plume in $F555W_0$. The error bars show the squareroot of the starcounts in each bin. Notice the dominance of the MS on WF2. In the more outlying fields, WF3 and WF4, the MS is much weaker.

Fig. 5b. – Luminosity functions along the red plume in $F814W_0$. The error bars show the squareroot of the starcounts in each bin. Notice how the red clump, located at $F814W_0 \approx 24$, has a smaller FWHM in the WF 3 and WF4 data compared with the PC1 and WF2 data.

Fig. 6.— Top: The V, I CMD of all stars on all chips. Bottom: I-band luminosity function

along the top of the red plume. The error bars shown reflect the squareroot of the starcounts in each bin. The magnitude of the TRGB from Tolstoy et al. (1998) based on ground-based, wide-field imaging is shown by the dashed line.

Fig. 7.— The V, I CMD of all stars with errors smaller than 0.2 mag. The Globular Cluster ridgelines of Da Costa & Armandroff (1990) are overlayed. $I_{TRGB,0}$ = 20.5 (see the dashed line) and $(m\text{-}M)_0$ = 24.5. The GCs and their metallicities, [Fe/H], are M 15, -2.17, NGC 6397, -1.91, M 2, -1.58, NGC 6752, -1.54, NGC 1851, -1.29, and 47 Tuc, -0.71.

Fig. 8.— The I-band luminosity function in the neighborhood of the red clump. The error bars shown reflect the squareroot of the starcounts in each bin. A fit which combines a linear part for the RGB and a Gaussian for the RC is overplotted. From this we determine $I_{RC,0}$ = 24.05.

Fig. 9.— Left: $[(V\text{-}I)_0, I_0]$ CMDs of all data with errors smaller than 0.1 mag in V and I. Right: $[(B\text{-}I)_0, I_0]$ CMDs of all data with errors smaller than 0.1 mag in B and I. The dotted lines at I_0 = 20.5 mark the observed location of the TRGB. The isochrones were matched to the observed TRGB (but since the AGB phase extends above the TRGB, this is not obvious from the plots). The data are overplotted with Z=0.0004 old and new Padua isochrones. The top panels show isochrones of young ages, the middle panels an isochrone of an intermediate age, and the bottom panels compare the data with a very old isochrone.

Fig. 10.— The $[(B\text{-}I)_0, I_0]$ CMD of Leo A. Only stars with errors of up to 0.1 mag are plotted. The dotted lines at I_0 = 20.5 mark the observed location of the TRGB. Yale isochrones for three ages and two metallicities are overplotted onto the data. They illustrate the age-metallicity degeneracy of the RGB. If the metallicity of the RGB stars is as high as that of the ISM of Leo A, then the age of the bulk of RGB stars is around ≈5 Gyr. Model RGB stars with metallicities slightly below that of stars in M 15 (the GC which empirically

describes the Leo A RGB) are slightly too blue, even for the oldest ages.

Fig. 11.— The [$(B\text{-}I)_0$, I_0] CMD of Leo A. Only stars with errors of up to 0.1 mag are plotted. The dotted lines at $I_0 = 20.5$ mark the observed location of the TRGB. Padua isochrones for three ages and two metallicities are overplotted onto the data. Frascati isochrones for Z=0.0001 are also overplotted for three ages. The RC/RHB requires stars no older than about 10 Gyr. The Frascati isochrones can match the RGB/AGB as well as the RC/RHB.

Fig. 12.— Top: The [$(V\text{-}I_0$, I_0] CMD of stars on the WF3 & WF4 chips. A few dashed lines are drawn to help compare the data with two models below. Middle: The baseline synthetic V, I CMD which results if we simply assume a constant SFR starting 12 Gyr ago and continuing on to the present. The differences between this model and the data guide us to a SFH which varies with time. Bottom: The SFH which produced most of the stars on the V, I CMD of the inner regions (Tolstoy et al. 1998) generates a red clump and giant branch morphology which is inconsistent with our data of the outer regions.

Fig. 13.— a.Top left: The [$(V\text{-}I_0$, I_0] CMD of stars on the WF3 & WF4 chips. Top right: The "best" synthetic V, I CMD that results from Model 1 ("no BHB"). Middle: Comparison of the data and the model in terms of their I-band LFs. Bottom: The SFH used to synthesize Model 1. The "zero" SFRs before the first, and between the first and the second event are real, in the sense that we do believe that the SFRs here were much smaller than either in the first or in the second event. The gap in SFR between the second and the third event is ill constrained.

Fig. 13b. – Top left: The [$(V\text{-}I_0$, I_0] CMD of stars on the WF3 & WF4 chips. Top right: The "best" synthetic V, I CMD that results from Model 2 ("maximum BHB"). Middle: Comparison of the data and the model in terms of their I-band LFs. Bottom: The SFH used to synthesize Model 2. Again, the gap in SFR between the second and the third event

is ill constrained.

5. Appendix A — Comparison with M 15

The purpose of this Appendix is twofold. First, a large body of data on GCs exists in B and V. We did not tap into this information in the main body of the paper, because we used the I-band TRGB to pin down the distance. Second, we wish to make a few remarks on the cluster distance scale, and how it affects the interpretation of Leo A data.

In Fig. A1, we show our best match of the M 15 [$(B\text{-}V)_0$, V_0] CMD to the Leo A [$(B\text{-}V)_0$, V_0] CMD (in an attempt to imitate the main-sequence-fitting technique). We used only the outlying fields of Leo A for this plot because the young component which overlaps a potential BHB is much weaker here. In Fig. A1, the solid lines for M 15 represent the data of Sandage (1970). The lines show the locations of the RGB, AGB, and HB of M 15 when shifted onto the Leo A data. The shift applied is 9.47 mag. This yields an excellent match to the RGB, AGB, RHB of Leo A. It also shows that some of the stars which are to the blue of the RGB can be interpreted as metal-poor AGB stars. Because the Sandage data are based on rather old, photoelectric photometry, we also constructed ridgelines using the CCD photometry of Durrell & Harris (1993). These are overplotted as dashed lines (after the same shift was applied). We see that there is about a 0.25 mag offset at the TRGB between the two data sets, but the overall fit is good. We also indicate where the RR Lyrae stars of M 15 (Silbermann & Smith 1995) are located when they are shifted by 9.47 mag[4]. These comparisons indicate that the distance modulus of Leo A is about 9.5 mag larger than that of M 15.

---

[4]Silbermann & Smith give a mean apparent V magnitude for the RR Lyr stars in M 15 of 15.82±0.03. Assuming an A_V of 0.31, then their dereddend V magnitude is 15.51. Dolphin et al. (2002) now find RR Lyr variables in Leo A with a mean V magnitude of 25.10±0.09. We assumed this was not extinction corrected, and applied an A_V of 0.068. We see that the difference in the magnitudes of the RR Lyr variables in M 15 and in Leo A is 9.52, in

Hipparcos observations of local subdwarfs have been used to re-derive the distances to Galactic GCs (Reid 1997, Reid & Gizis 1998, Reid 1999). We notice that one effect of the new GC distances is to shift the absolute I-band TRGB magnitudes of Da Costa & Armandroff (1990), which are commonly used to derive distances to external galaxies. These shifts are not in concert. Relative shifts in GC distances conspire to introduce a larger dispersion of M_I at the TRGB than the pre-Hipparcos distances had indicated. With the post-Hipparcos distances to GCs, the error associated with the TRGB method increases. (We estimate that the dispersion is now 0.2, rather than 0.1 mag, in M_I. But note that Reid (1999) gives an uncertainty of at least $\pm$0.1 mag in post-Hipparcos cluster distance moduli.) Similarly, since Da Costa & Armandroff calibrate metallicity against V-I color, metallicities and metallicity errors derived based on GC ridgelines change when the new cluster distances are adopted. More importantly, however, the absolute distance modulus of M 15 has been re-calibrated in the post-Hipparcos era. Reid (1997) gives $(m\text{-}M)_0$=15.38, while Da Costa & Armandroff (1990) assumed $(m\text{-}M)_0$=15.10. Therefore, the Leo A distance modulus is 24.9 using the new M 15 distance, and 24.6 using the old M 15 distance.

In principle there are two sources of error for the distance modulus coming from the calibration, once M 15 has been chosen as the standard candle. One is related to the relative modulus between M 15 and Leo A; the other comes from the modulus adopted for M 15. Reid (1999) quotes an uncertainty of at least $\pm$0.1 mag in the cluster distance moduli. The error in the relative modulus between M 15 and Leo A has two components. One arises from the difference between the two M 15 data sets at the TRGB, $\pm$0.13 mag, which most probably results from different sampling at the TRGB. Uncertainty in the sampling of the

---

excellent agreement with the value we derive from shifting M 15's RGB, AGB, and HB onto the Leo A CMD.

Leo A TRGB adds at least another 0.1–0.2 mag. Therefore, the total error on the distance modulus of Leo A as derived from comparison with M 15 is $\approx\pm0.2$.

The large distance to Leo A which results when one adopts the new distance of M 15 does not change our main conclusions. We detect old and metal-poor RHB stars. Therefore, Leo A cannot be younger than 2 Gyr. However, the material presented in this Appendix serves to illustrate the difficulty in disentangling distance, metallicity, and age from one another, when neither one is known with certainty.

Fig. A1. – The [$(B\text{-}V)_0$, V_0] CMD of the WF3 & 4 chips. Only stars with errors in B and V of up to 0.1 mag are plotted. We overplot two ridgeline sets for M 15. The solid lines give the RGB, AGB and HB after Sandage (1970), shifted by 9.47 mag. To verify the locations with modern data we also constructed an RGB and a BHB ridgeline from the data of Durrell & Harris (1993); these are the dashed lines. The small cross shows the location of RR Lyrae variables in M 15 after Silbermann & Smith (1995).

This figure "sl_leoa_Fig1.jpg" is available in "jpg" format from:

http://arXiv.org/ps/astro-ph/0205052v1


This figure "sl_leoa_Figa1.jpg" is available in "jpg" format from:
http://arXiv.org/ps/astro-ph/0205052v1


This figure "sl_leoa_Fig2a.jpg" is available in "jpg" format from:
http://arXiv.org/ps/astro-ph/0205052v1


This figure "sl_leoa_Fig2b.jpg" is available in "jpg" format from:
http://arXiv.org/ps/astro-ph/0205052v1

This figure "sl_leoa_Fig2c.jpg" is available in "jpg" format from:

http://arXiv.org/ps/astro-ph/0205052v1


This figure "sl_leoa_Fig3.jpg" is available in "jpg" format from:
http://arXiv.org/ps/astro-ph/0205052v1

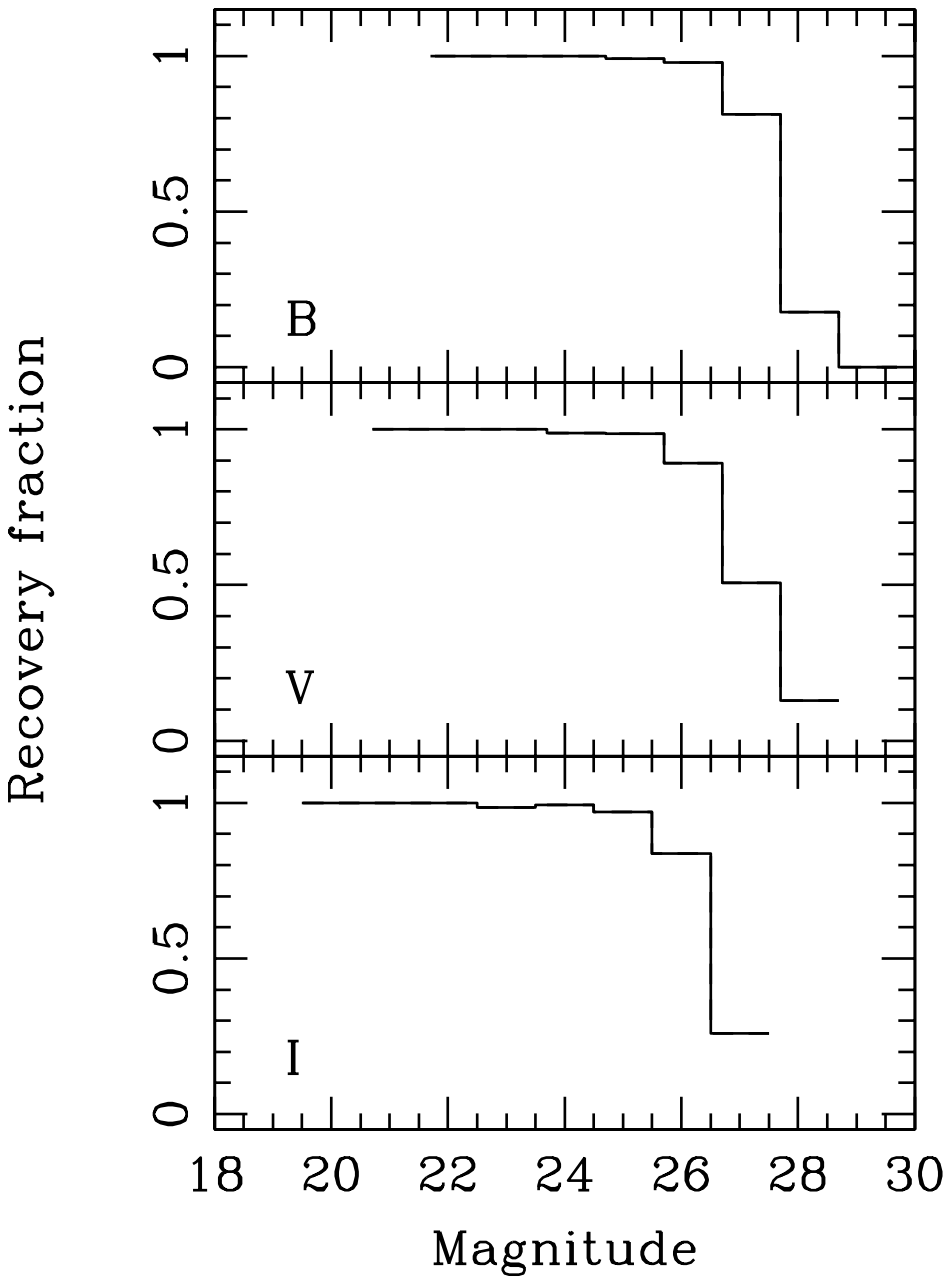
Recovery fraction
0
0.5
1
0
0.5
1
0
0.5
1
B
V
I
18
20
22
24
26
28
30
Magnitude

This figure "sl_leoa_Fig5a.jpg" is available in "jpg" format from:

http://arXiv.org/ps/astro-ph/0205052v1


This figure "sl_leoa_Fig5b.jpg" is available in "jpg" format from:
http://arXiv.org/ps/astro-ph/0205052v1


This figure "sl_leoa_Fig6.jpg" is available in "jpg" format from:
http://arXiv.org/ps/astro-ph/0205052v1


This figure "sl_leoa_Fig7.jpg" is available in "jpg" format from:
http://arXiv.org/ps/astro-ph/0205052v1

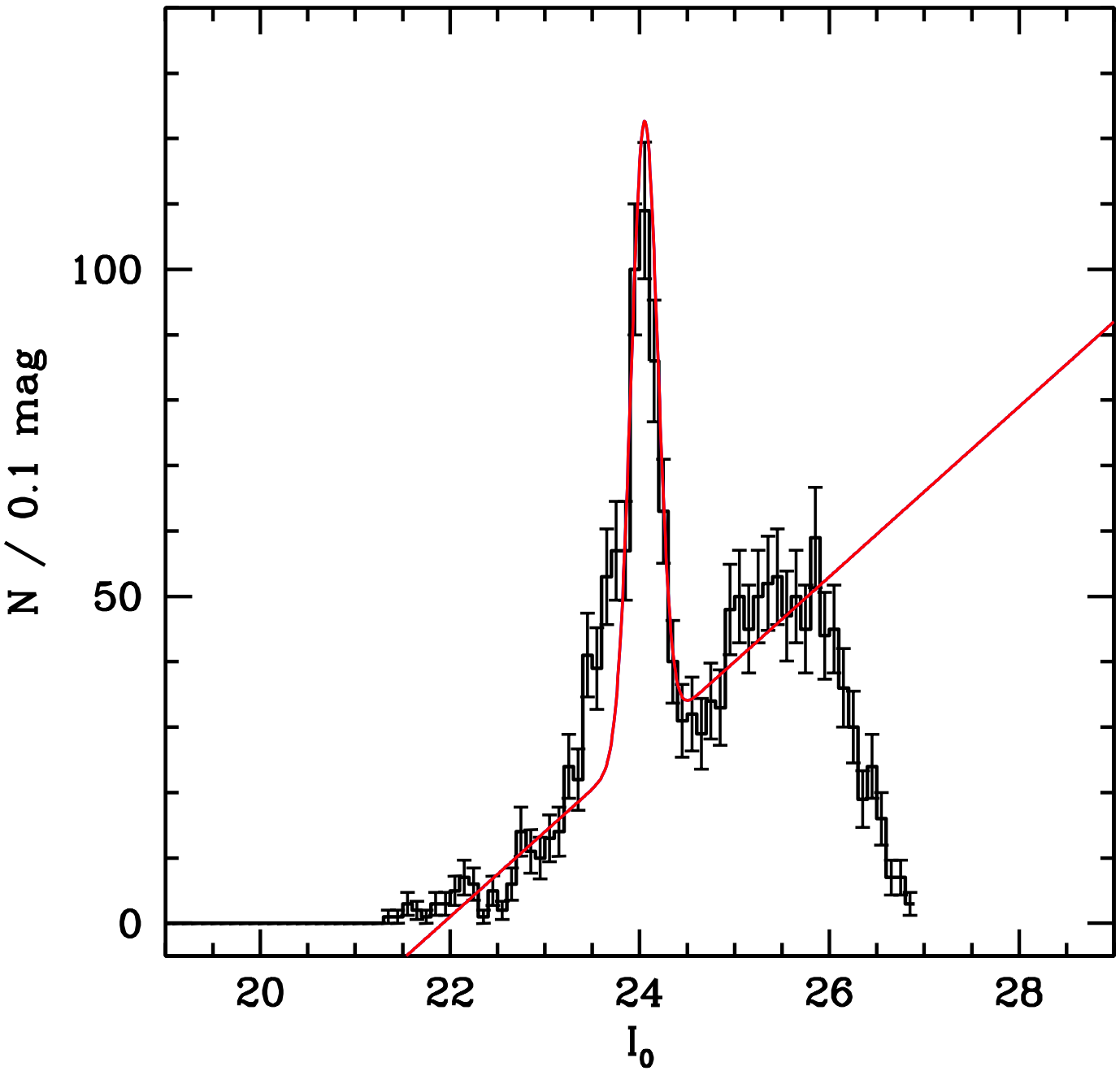
N / 0.1 mag
100
50
0
20
22
24
26
28
I0


This figure "sl_leoa_Fig9.jpg" is available in "jpg" format from:
http://arXiv.org/ps/astro-ph/0205052v1


This figure "sl_leoa_Fig10.jpg" is available in "jpg" format from:
http://arXiv.org/ps/astro-ph/0205052v1


This figure "sl_leoa_Fig11.jpg" is available in "jpg" format from:
http://arXiv.org/ps/astro-ph/0205052v1


This figure "sl_leoa_Fig12.jpg" is available in "jpg" format from:
http://arXiv.org/ps/astro-ph/0205052v1


This figure "sl_leoa_Fig13a.jpg" is available in "jpg" format from:
http://arXiv.org/ps/astro-ph/0205052v1


This figure "sl_leoa_Fig13b.jpg" is available in "jpg" format from:
http://arXiv.org/ps/astro-ph/0205052v1